IEEE Access
Multidisciplinary ⋮ Rapid Review ⋮ Open Access Journal

Received 17 July 2024, accepted 26 August 2024, date of publication 30 August 2024, date of current version 20 September 2024.

Digital Object Identifier 10.1109/ACCESS.2024.3452185

RESEARCH ARTICLE

A Flexible Conformal Phased Array With Embedded Magnetic Particles Based Composite Right/Left Handed Metamaterial Phase Shifters

MUHAMMAD AYAZ[1], IRFAN ULLAH[1], ADNAN IFTIKHAR[2], (Senior Member, IEEE), SYED MUZAHIR ABBAS[3], (Senior Member, IEEE), BENJAMIN D. BRAATEN[4], (Senior Member, IEEE), SHAHID KHATTAK[1], AND MOATH ALATHBAH[5]

[1]Department of Electrical and Computer Engineering, COMSATS University Islamabad, Abbottabad Campus, Abbottabad 22060, Pakistan
[2]Department of Electrical and Computer Engineering, COMSATS University Islamabad, Islamabad Campus, Islamabad 45550, Pakistan
[3]School of Engineering, Faculty of Science and Engineering, Macquarie University, Sydney, NSW 2109, Australia
[4]Department of Electrical and Computer Engineering, North Dakota State University, Fargo, ND 58102, USA
[5]Department of Electrical Engineering, College of Engineering, King Saud University, Riyadh 11451, Saudi Arabia

Corresponding authors: Adnan Iftikhar (adnaniftikhar@comsats.edu.pk) and Irfan Ullah (eengr@cuiatd.edu.pk)

This work was supported by Researchers Supporting Project number (RSPD2024R868), King Saud University, Riyadh, Saudi Arabia and by the Higher Education Commission (HEC)-National Research Program for Universities (NRPU), Pakistan, via Project No. 20-14696/NRPU/RD/HEC/2021.

ABSTRACT In this study, a flexible and fully printable four element patch antenna array bent on a cylindrical-shaped surface for main beam steering is proposed. The individual phases of the microstrip patches in the array are varied by using novel planar phase shifters constituted of microstrip composite right/left-handed (CRLH) lines ingrained with microparticles. The reinforcement of newly introduced microparticles in the CRLH transmission line structure makes it a variable phase shifter, which is fabricated on a flexible substrate in completely planar and conformal configurations. The magnetic particles-based CRLH-TL phase shifter (MP-CRLH) consists of multiple cavities in the substrate filled with micron-sized silver-coated ferrite particles. These particles in the cavity are magnetically aligned by a small magnet placed beneath the cavity. A particular phase shift can be achieved by activating particles in multiple cavities in the MP-CLRH phase shifter. The optimum locations of the cavities partially filled with magnetic particles for a particular phase shift have been explored after extensive 3D simulations in the frequency domain using CST Studio Suite. The main advantage of using the MP-CRLH phase shifter is that it can be conformed to non-planar surfaces, such as cylindrical-shaped in this scenario. As compared to conventional IC/discrete components-based phase shifters, the working of the novel MP-CRLH phase shifter is independent of external SMT and lumped circuit components for its biasing. The four unit-cell cascaded MP-CRLH phase shifter is then integrated with a four-element patch array on a cylindrical-shaped surface with radii of 30 cm and 10 cm. The main pattern of the array has been successfully scanned at 0°, −15°, and +30° using the integrated MP-CRLH phase shifter at.2.45 GHz. The full-wave simulation results are validated with the measured radiation patterns in a fully anechoic chamber facility. The conformal phased array integrated with MP-CRLH phase shifters on a flexible substrate can be used for applications like on-body communication systems, wearable devices, flexible electronics, and aircraft communication systems.

INDEX TERMS Microparticles, nanoparticles, composite right/left-handed (CRLH) transmission line conformal antenna, antenna array, flexible substrate.

The associate editor coordinating the review of this manuscript and approving it for publication was Wanchen Yang.

I. INTRODUCTION

Conformal antenna arrays are designed to fit seamlessly onto curved surfaces and have shown a wide range of

applications in various technological fields such as aerospace, satellites, defense, and medical. Such phased arrays enable healthcare innovations, Internet of Things (IoT) devices, and peripheral technology by providing seamless connectivity in a wireless society. Their versatility optimizes signal performance, defining a new era of high-performance wireless technology from automotive communication to consumer flexible electronics. In addition, they are very environment-friendly, space-efficient and easy to install [1]. One significant feature of conformal arrays is their beam steering capability, which is of the utmost importance in conformal antennas for micro base stations and aircraft communication systems that require wide angle radiation coverage. They have the capability to scan the main beam in the desired direction, which has tremendous application potential for installation on non-planar platforms with wide angular coverage [2], [3], [4], [5], [6].

The relevant research work to achieve main beam scanning using conformal antenna arrays has been presented in this section. In [7] and [8], PIN didoes are incorporated in feed networks to achieve the desired phases for beam switching and scanning. Due to the switching characteristic of PIN diodes, the desired phase of the signal can change in the feeding network of the antenna array. Similarly, the tunable capacitance characteristic varactor diodes have been used to achieve the desired phases to realize the antenna array beam scanning. The primary disadvantage of utilizing PIN diodes in conformal arrays is that external biasing circuitry and DC voltage are required. This type of circuitry is not suitable for smooth integration on a conformal surface due to the discrete nature of the diodes. Recently, in [9], a beam scanning conformal antenna array with a planar integrated phase shifter based on graphene was proposed. The overall design consists of two printed dipole elements, a microstrip power divider, feed baluns, and a fork-shaped distributed capacitor, using a graphene flake as a phase shifter. By varying the resistance of the graphene flake, the antenna array can achieve beam scanning at 7.2 GHz. The design, which has been fabricated and tested, holds promise for future use in flexible electronics. The drawback of this work includes the requirement of an external voltage to change the resistance of graphene material. In [10], a 1×4 phased antenna array at 4.99 GHz is studied using a flexible substrate, Kapton polyimide. An inkjet 2-bit phase shifter is used with carbon nanotube thin-film transistors as switching elements. The array's main beam is scanned from $0°$ to $-27°$. Using carbon nanotube thin-film transistors and ink-jet phase shifters in a flexible substrate are innovative techniques, but these have potential limitations, including high manufacturing costs, challenges in scaling up production due to complexity, and concerns about long-term reliability in harsh conditions. Similarly, in [11], a phased antenna array is designed using multilayer graphene film in the feeding network. A butler matrix is designed to achieve the desired phases for large beam scanning of $120°$. However, using multilayer graphene film in the feeding network has potential drawbacks, which include challenges related to the graphene layer uniformity and quality, potential limitations in scalability, and concerns regarding the implementation complexity of the butler matrix for achieving large beam scanning angles in conformal phased arrays. A millimeter wave Vivaldi antenna is presented for radiation beam scanning at $90°$ and $270°$ in [12]. In this work, a graphene-based tunable resistor is used to scan the main beam in a particular direction. However, the potential limitation includes the requirement of external voltage to change the resistance of graphene-based tunable resistor. In [13], a millimeter-wave conformal antenna array has been presented at 61 GHz for main beam steering applications. For switching purposes, a single-pole three-throw semiconductor switch is used. The proposed array is bent on a cylindrical surface with a radius of 25 cm for beam switching of $-32°$ to $34°$. The SP3T semiconductor switch used in the prototype has some potential challenges, which include its power handling and heat dissipation. A conformal dipole antenna array has been investigated with four branches at 2.7 GHz with maximum main beam scanning of $\pm 60°$ in [14]. In this work, three metallic strip directors are used to increase the gain of the proposed antenna array. The addition of metallic strip directors complicates the antenna design. This complexity can increase manufacturing costs and necessitate the use of specialized equipment and materials.

In this proposed work, a 1×4 flexible conformal phased array integrated with innovative magnetic particles based composite right-left hand (MP-CRLH) inspired phase shifters is designed for main lobe steering applications. The patch antenna array and MP-CRLH phase shifters have been designed on a single flexible substrate (Rogers RT5880) at 2.45 GHz. The flexible phase shifter section in the conformal phased array consists of inter-digital capacitors (IDCs) and stub inductors (SIs) with cavities in the substrate. The cavities filled with silver-coated micron-sized ferrite particles are drilled under the stub section. By activating these magnetic particles in multiple cavities in the MP-CRLH phase shifter, the desired scanning phase can be obtained for main beam steering. The potential benefits of choosing the CRLH structure with the magnetic particles are: (i) it enables multi band operation and has a more compact size compared to conventional TL-based phase shifters due to its negative phase response in the left-handed mode; (ii) by incorporating MP into the stub's inductors of the CRLH-TLs, a fraction of the power can pass through a single cavity, significantly enhancing the phase shifter's power handling capacity; (iii) the proposed MP-CRLH has been chosen to maintain a constant phase shift, high return loss, and low insertion loss; and (iv) the use of MP embedded in CRLH transmission line to achieve variable phase shifters offer a wide range of applications, including radar, satellite communication, and possible integration with non-planar microwave electronics devices, whereas traditional chip-based phase shifters require

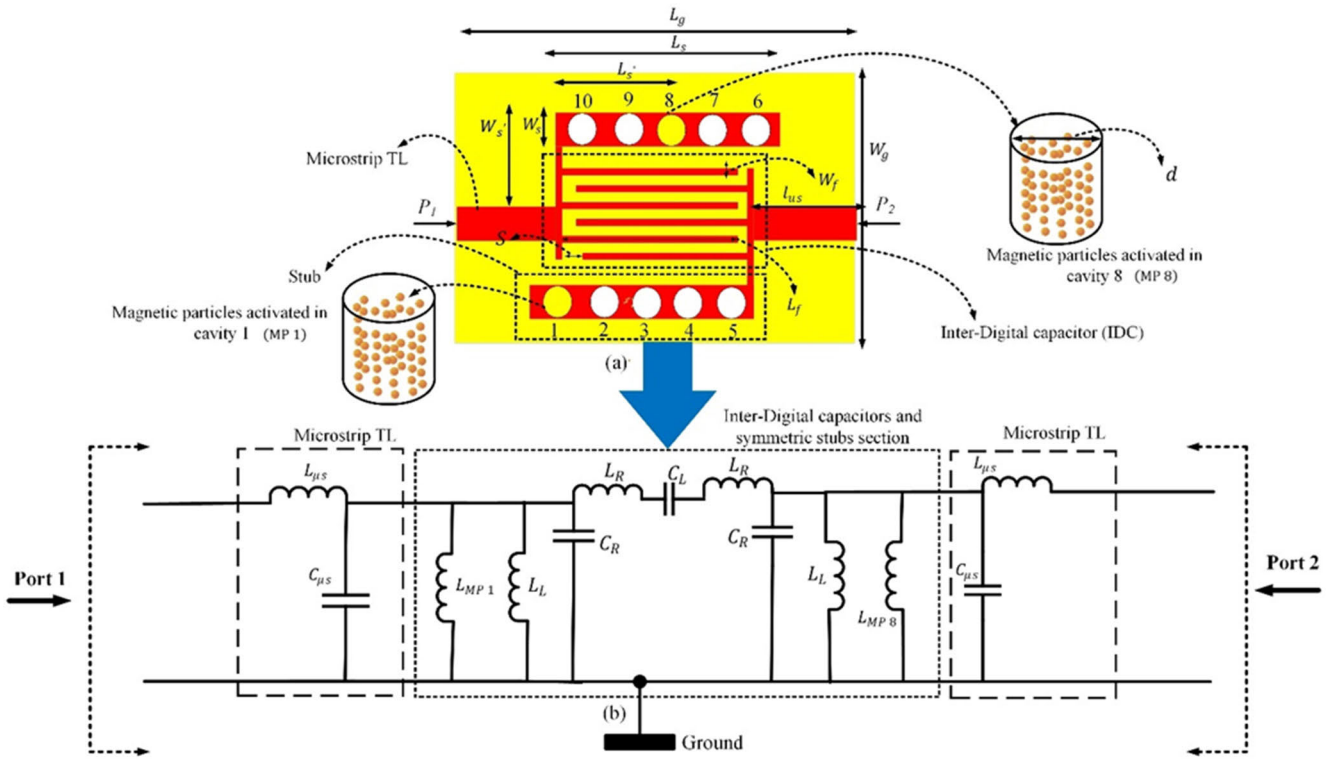

FIGURE 1. The proposed MP-CRLH phase shifter (a) unit-cell schematic figure, (b) unit-cell equivalent electrical circuit model.

DC voltage and have limitations of external biasing circuitry. Similarly, the key advantages of this flexible phased array integrated with cascaded MP-CRLH phase shifters are: (i) reduce overall complexity; (ii) no need for an external biasing circuitry; (iii) fully flexible and can be conformed to any conformal surface; (iv) fully printed, that is, the antenna and phase shifter are designed on the same PCB; and (v) no requirement for transmission line discontinuity to achieve the desired phase shift.

The layout of the paper is as follows: The detailed design and analysis of the unit-cell MP-CRLH phase shifter are presented in Section II. In Section III, the design and working mechanism of the flexible conformal phased array using the CST Microwave Studio Suite are presented. Section IV demonstrates the measurement setup and result validation. Finally, Section V gives the conclusion and future research perspectives.

II. DESIGN OF MAGNETIC PARTICLES (MP) INSPIRED CRLH PHASE SHIFTER

A. UNIT-CELL MP-CRLH PHASE SHIFTER

The layout of a unit-cell MP-CRLH phase shifter is shown in Figure 1 (a). The proposed phase shifter is designed at 2.45 GHz on a Rogers RT5880 substrate ($\varepsilon_r = 2.2$, $tan\delta = 0.0009$ and thickness=1.575 mm).

The unit cell structure comprises a microstrip inter-digital capacitor (IDC) with three pairs of capacitive fingers, each with a length of L_f and a width of W_f, and a spacing of S between the fingers. The IDC is connected with two symmetrical stub transmission lines, each having a length of L_s with width W_s. The ten cavities (numbered 1 to 10) are made under both symmetric stub transmission lines.

Each stub line consists of five cavities, with spacing d among the cavities. Then partial filling of these cavities is served with silver-coated ferrite magnetic particles (SM25P20 SILVER FERRITE in [19]).Two small sections of printed microstrip lines are connected on both ends of the IDC for impedance matching. The resulting proposed phase shifter is referred to as the magnetic particles composite right/left-handed (MP-CRLH) phase shifter. The working principle of the MP-CRLH phase shifter is explained as follows: A small, tiny magnet is placed beneath any cavity, which aligns the micron-sized magnetic particles in the cavity. For illustration purposes, the alignment of particles in cavities 1 and 8 (MP1 and MP8) is shown in Figure 1(a). In this case, the effective length of the upper stub line is $L_{s'}$, while that of the lower stub is L_s. As a result, the inductances of both the stub transmission lines are changed, which changes the overall inductance of the structure and also changes other parameters of the structure due to the composite nature of the CRLH line. This finally results in changing the structural parameters of the CRLH transmission line, and, hence changing the phase shift of the RF signal propagating from port 1 to port 2.

Therefore, the desired phase shift of the RF signal can be achieved by activating the magnetic particles in an appropriate cavity or combination of cavities. The optimized

designing parameters (in mm) for the ISM band are: (L_S = 8, W_S = 2, W_f = 0.3, L_f = 6, d = 1, and S = 0.2). These dimensions were obtained in a full-wave CST simulator using the design guidelines in [16], [17], [18], [19], [20], [21], and [22]. The equivalent electrical circuit model of the proposed MP-CRLH phase shifter is shown in Figure 1 (b). The inductance and capacitance of the phase shifter's small microstrip sections on both ends are represented by $L_{\mu s}$ and $C_{\mu s}$. The four structural parameters of the conventional CRLH transmission line are C_L, L_L, L_R and C_R with additional inductance of magnetic particles is represented by L_{MP}. The circuit parameters C_L, L_L, L_R and C_R are calculated using the following expressions [23]:

$$C_L = (\varepsilon_r + 1)\, L_f \left\{ 4.409\,(N-3) \tanh\left[0.55 \left(\frac{h}{W_f} \right)^{0.45} \right] + 9.92 \tanh\left[0.52 \left(\frac{h}{W_f} \right)^{0.5} \right] \right\} \times 10^{-12} \quad (1)$$

$$L_L = \frac{\mu_0}{2\pi} \left[h.\ln\left(\frac{h + \sqrt{r^2 + h^2}}{r} \right) + \frac{3}{2}\left(r - \sqrt{r^2 + h^2} \right) \right] + \frac{Z_{stub}\sqrt{\varepsilon_{re}}}{c_0} L_{s'} + \frac{Z_3\sqrt{\varepsilon_{re}}}{c_0} W_{s'} \quad (2)$$

$$L_R = \frac{1}{N} \frac{Z_{IDC}\sqrt{\varepsilon_{re}}}{c_0} L_f \quad (3)$$

$$C_R = \frac{N}{2c_0} \frac{\sqrt{\varepsilon_{re}}}{Z_{IDC}} L_f \quad (4)$$

$$C_{\mu s} = \sqrt{\varepsilon_{re}}/(c_0 Z_{\mu s}) \quad (5)$$

$$L_{\mu s} = Z_{\mu s}^2 C_{\mu s} \quad (6)$$

where ε_r is the dielectric constant of the substrate material, ε_{re} is the effective dielectric constant, c_0 is the speed of light, N is the number of finger pairs in IDC and h is the thickness of the substrate. r is the radius of the cavity, $L_{s'}$ is the effective stub length corresponding to activated cavity (for example, if cavity 1 is activated, then $L_{s'} = L_s$, and if suppose cavity 8 is activated, then $L_{s'} < L_s$), $W_{s'}$ is the height of the stub line, $Z_{\mu s}$, Z_{IDC}, Z_{stub} and Z_3 are the characteristic impedances of the short microstrip sections, IDC fingers, effective stub length, and the connecting line length corresponding to $W_{s'}$ respectively.

The inductance L_{MP} of the activated magnetic particles in cavity can be calculated using [24]

$$L_{MP} = \frac{\mu_0}{2\pi} \left[h.\ln\left(h\ln\left(\frac{2h + \sqrt{r^2 + h^2}}{r} \right) + \frac{3}{2}\left(r - \sqrt{r^2 + h^2} \right) \right) \right] \quad (7)$$

The propagation constant for a balanced CRLH transmission line is given by [16]

$$\beta = \omega\sqrt{L_R C_R} - \frac{1}{\omega\sqrt{(L_{MP}||L_L)C_L}} \quad (8)$$

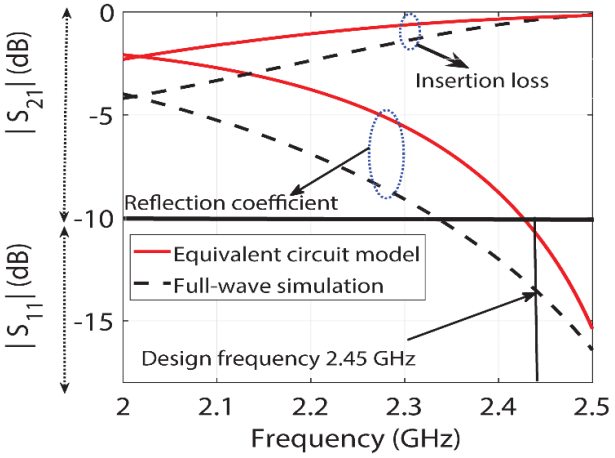

FIGURE 2. Simulated reflection coefficient and insertion loss of the unit-cell MP-CRLH phase shifter at 2.45 GHz.

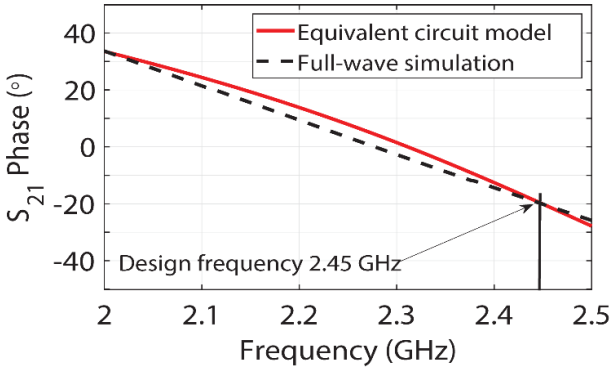

FIGURE 3. Simulated phase response of the unit-cell MP-CRLH phase shifter at 2.45 GHz.

The resulting phase shift to the input signal from port 1 to port 2 introduced by the MP-CRLH phase shifter in Figure 1 is simply calculated as

$$\phi_{21}^{\text{MP-CRLH}} = -\beta L_s \quad (9)$$

and the phase shift contribution due to microstrip sections is given by [25]

The total phase shift from port 1 to port 2 is therefore can be written as

$$\phi_{21}^{total} = \phi_{21}^{\text{MP-CRLH}} + \phi_{21}{}^{\mu s} \quad (10)$$

where L_s is the length of MP-CRLH phase shifter and $l_{\mu s}$ is the length of short microstrip lines in Figure 1. If the MP-CRLH phase shifter unit cell is cascaded with M sections, the total MP-CRLH phase shift will simply be $M\phi_{21}^{total}$. Based on the above equivalent circuit analysis, the MP-CRLH phase shifter is designed at frequency of 2.45 GHz using equations (1)-(7) with following calculated circuit values C_L = 2.64 pF, L_L = 1 nH, L_R = 1.1 nH, C_R = 2.7 nH, $C_{\mu s}$ = 1 pF, $L_{\mu s}$ = 0.75 nH and L_{MP} = 4.5 nH. For full-wave simulation, the flexible Rogers substrate RT5880 (ε_r = 2.2, $tan\delta$ = 0.0009 and thickness h = 1.575 mm) is used with

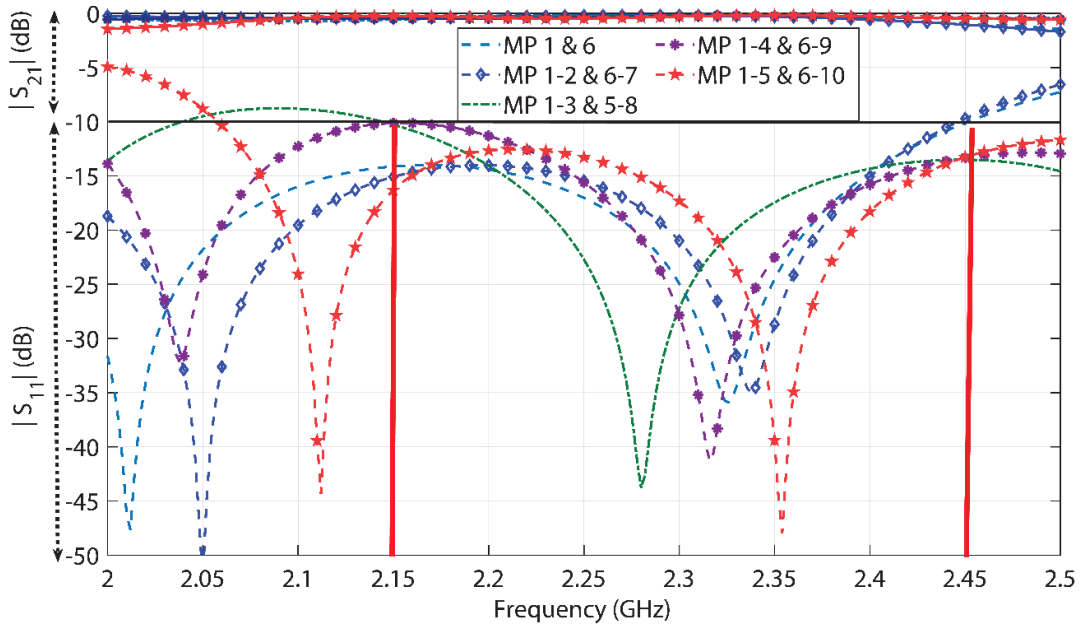

FIGURE 4. Cascaded MP-CRLH phase shifter reflection coefficients and insertion losses in planar configuration for multiple activated magnetic particles (MPs).

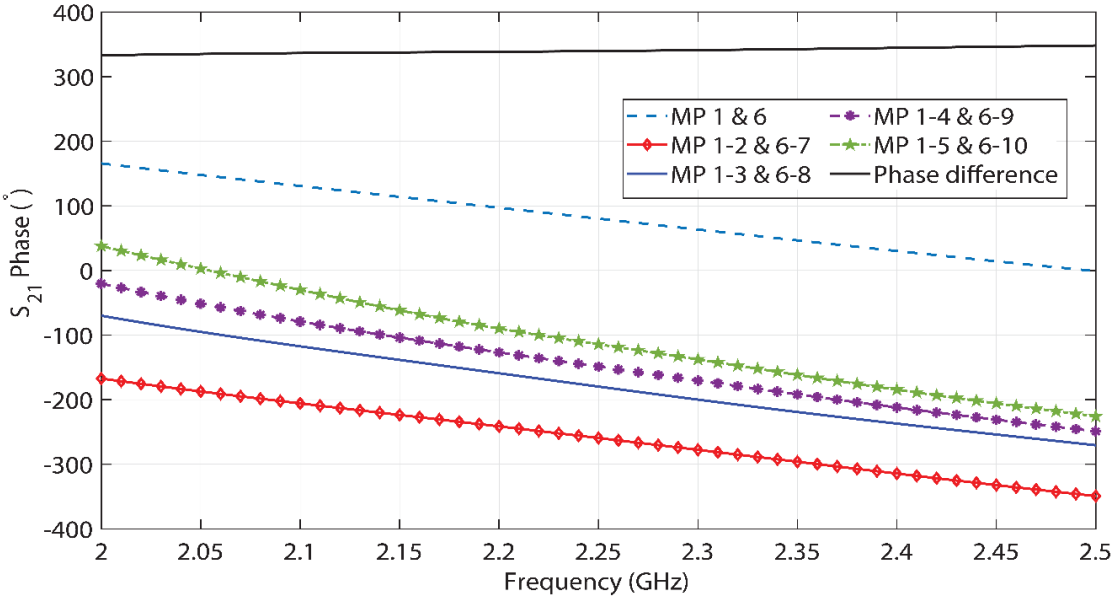

FIGURE 5. Cascaded MP-CRLH phase shifter phase responses in planar configuration for multiple activated MPs.

particles in cavities 1 and 6 aligned. Figure 2 depicts the equivalent circuit modeling and full-wave simulation results for the proposed phase shifter. At the design frequency of 2.45 GHz, the reflection coefficient is less than 10 dB and insertion loss are one dB as shown in Figure 2. At 2.45 GHz, the phase shift is $-20°$ for both circuit modeling and full-wave simulation, as depicted in Figure 3. The results validate the accuracy of circuit-level modeling using (1)–(10). Next, to extend the range of phase shifts, four unit-cell MP-CRLH phase shifters in Figure 1 are cascaded and are discussed in the next section.

B. PLANAR FOUR UNIT-CELL CASCADED MP-CRLH PHASE SHIFT

The MP-CRLH phase shifter unit cell shown in Figure 1 is cascaded to four unit cells in the full-wave CST simulator for magnetic particles (MP) activation in various cavities. The resulting full-wave simulated results for the magnitudes of reflection coefficients ($|S_{11}|$) and insertion losses ($|S_{21}|$) are shown in Figure 4. The $|S_{11}| < -10$ dB with insertion loss $|S_{21}| \cong 0.2 - 0.5$ dB in the ISM band ($2 - 2.5$ GHz) for the MPs activation in various cavities. The corresponding phase response is shown in Figure 5. The maximum achieved

phase difference is 340° with the cascaded configuration, and it is flat over the entire frequency band. As observed in Figure 5, maximum phase difference is 340°, whereas the phase range can be extended to 360° by extending the stub length for additional holes to add MPs and use longer IDCs to retain symmetry of the MP-CRLH structure. For the demonstration of the MP-CRLH phase shifter on conformal beam scanning applications with scan angle is +30°, the MP-CRLH structure shown above with 340° phase range gives the appropriate phases to each antenna element. After achieving the maximum phase shift, the cascaded planar MP-CRLH is conformed on to cylindrical conformal surfaces with *radii* = 30 cm and 10 cm for phase response analysis in the next section.

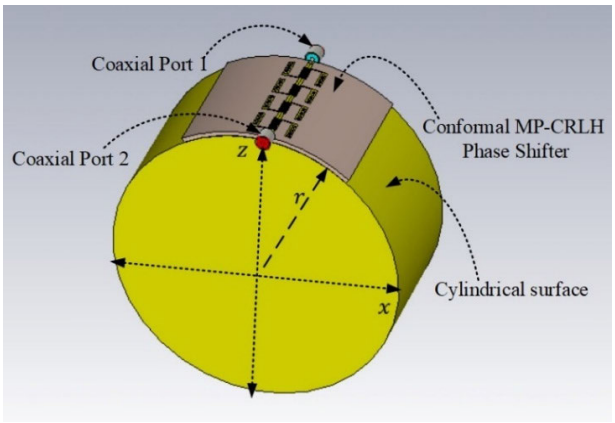

FIGURE 6. Cascaded MP-CRLH phase shifter conformed on a cylindrical-shaped surface with radius r.

C. CONFORMAL FOUR UNIT-CELL CASCADED MP-CRLH PHASE SHIFTER

In this section, the planar MP-CRLH phase shifter is conformed on a cylindrical-shaped surface with radius r in CST simulator to evaluate its performance on a conformal surface, as illustrated in Figure 6.

Initially the conformal phase shifter is tested at 2.45 GHz on a larger cylindrical surface with radius 30 cm, and subsequently on a smaller with radius 10 cm surface. For both surfaces, the MP-CRLH phase shifter consistently maintains crucial performance with $|S_{11}| < -10$ dB and maximum insertion loss $|S_{21}| \cong -3$ dB within the frequency range of 2 − 2.5 GHz. The achieved $|S_{11}|$ (dB) and $|S_{21}|$ (dB) are depicted in Figures 7 and 9 for $r = 30$ cm and $r = 10$ cm cylindrical conformal surfaces, respectively. The corresponding linear phase responses for the MPs activation in the simulation model are shown in Figures 8 and 10. The phase response of the MP-CRLH phase shifter on conformal surfaces is closely matched with that of the MP-CRLH phase shifter on planar surfaces. The maximum phase shift achieved on $r = 30$ cm conformal surface is 340°, which is the same as that achieved on a planar surface (see Figure 5). However, there is 50° variation in the maximum phase shift on $r = 10$ cm surface over the desired operating band. The variations are due to severe surface deformation on $r = 10$ cm conformal surface as compared to $r = 30$ cm surface. The results show that the proposed conformal MP-CRLH phase shifter may operate with minimal variations in phase response on both planar and conformal surfaces with less than 10 cm of surface deformation.

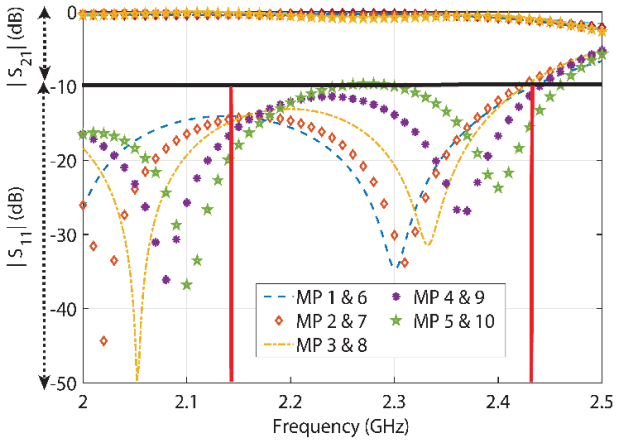

FIGURE 7. Conformed MP-CRLH phase shifter reflection coefficients and insertion losses on cylindrical surface with radius r = 30 cm for multiple activated MP.

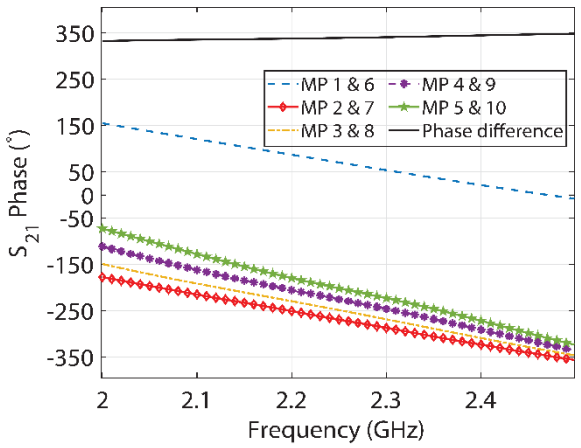

FIGURE 8. Conformed MP-CRLH phase shifter phase response on cylindrical surface with radius r = 30 cm for multiple activated MP.

The root-mean-square (rms) magnitude and phase errors of the proposed cascaded MP-CRLH for different phase shift values is also computed to observe the maximum in-band phase error and amplitude imbalance, respectively. Figure 11 displays the rms magnitude, whereas Figure 12 shows the rms phase error, of the proposed cascaded MP-CRLH phase shifters at phase shifter values 50°, 100°, 200°, and 300°. It can be observed that maximum phase error within the band i.e. from 2.15 to 2.45 GHz, is below 18°. Similarly, the amplitude imbalance is less than 1 dB over frequency range from 2.15 to 2.45 GHz.

In the next section, the conformal phase shifter is integrated with a 1 × 4 flexible phased array on the same substrate. Following the achievement of the desired

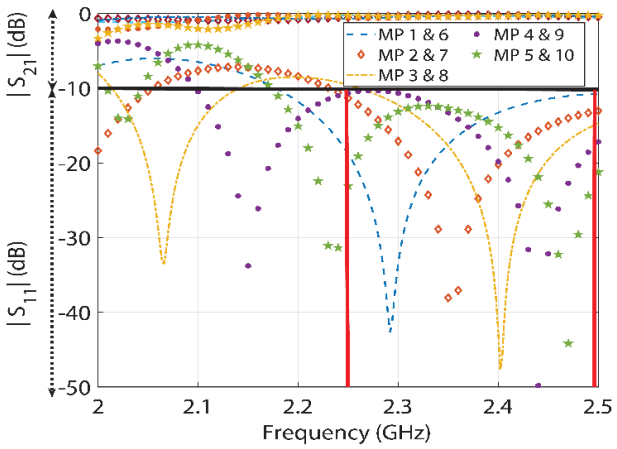

FIGURE 9. Reflection coefficients and insertion losses of a conformal MP-CRLH phase shifter on cylindrical surface with radius $r = 10$ cm for multiple activated MP.

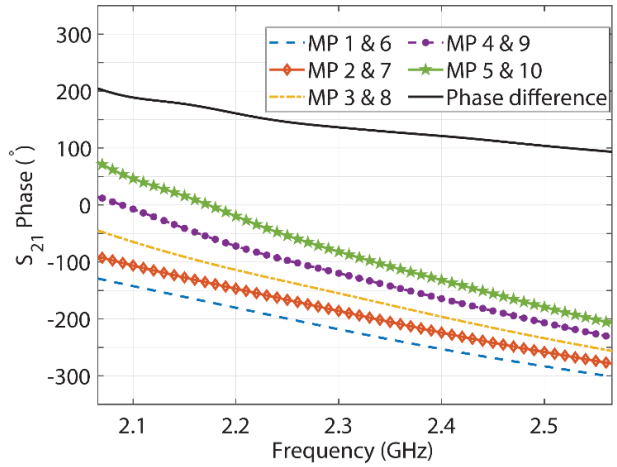

FIGURE 10. Conformed MP-CRLH phase shifter phase response on cylindrical surface with radius r = 10 cm for multiple activated MP.

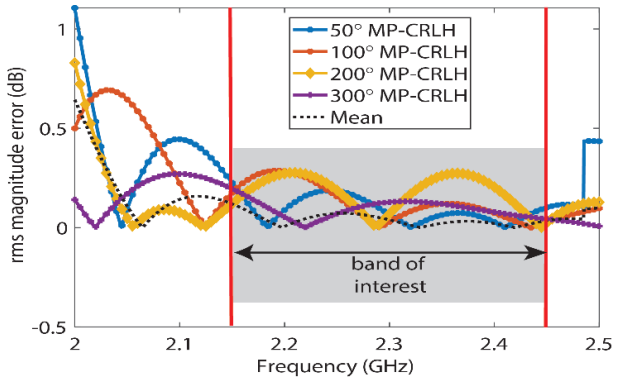

FIGURE 11. In band rms magnitude error of the proposed MP-CRLH at different phase shifter values.

phases in the coupled environment for the main lobe scanning, the cascaded MP-CRLH phase shifter demonstrated the capability to excite the antenna elements in planar as well in conformal scenario for phased array applications.

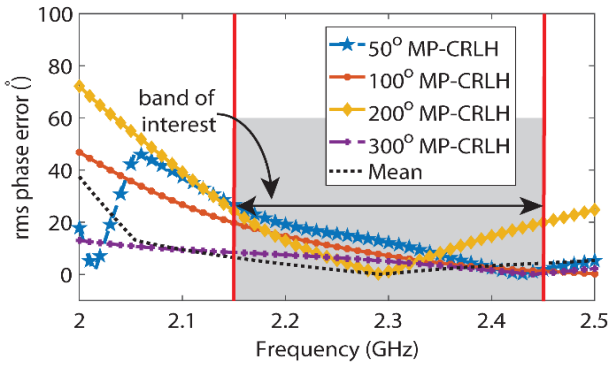

FIGURE 12. In band rms phase error of the proposed MP-CRLH at different phase shifter values.

III. FULL WAVE SIMULATION RESULTS OF FLEXIBLE CONFORMAL PHASED ARRAY EXCITED WITH MP-CRLH PHASE SHIFTERS

In this section, a full-wave simulation model of a four-element cylindrical antenna array integrated with flexible conformal MP-CRLH phase shifters shown in Figure 13 is presented to achieve main beam steering. For simulation purposes, the 3D EM simulation software CST Microwave Studio Suit 2019 version is used in the frequency domain. In the simulation setting, 100 number of passes are used, whereas 2000 number of iterations are used. Silver-coated spheres were placed on the bottom of the MP-CRLH phase shifter cavities in simulations to simulate the particles in the OFF state and to mimic the absence of the magnetic field. In contrast, 28 columns of the silver-coated spheres were modeled in the simulation with an average diameter of 25 microns to establish a connection between the particles at the cavity bottom and the stub inductor. This arrangement represented the presence of the magnetic field. A parametric analysis was also performed on the number of columns of modeled magnetic particle spheres to examine the changes in S-parameters and to minimize the simulation time. It was found that two columns of particles resulted in identical results to those 25 columns: however, two columns in the cavity significantly reduced design complexity and simulation time [24], [26], [27], [28], [29], [30].

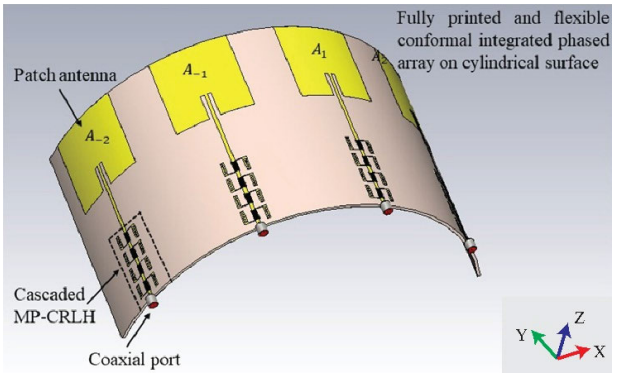

FIGURE 13. Full-wave simulation model of 1 × 4 flexible conformal array with integrated MP-CRLH phase shifters.

Three cases of full-wave simulations for a four-element patch array with embedded MP-CRLH phase shifters are shown in Figure 13. Planar arrays and flexible conformal arrays on cylinders with radii of $r = 30$ cm and $r = 10$ cm. The three cases are simulated for inter-element spacing of $\lambda/2$ at $f = 2.45$ GHz.

In order to observe the mutual coupling effect of the antenna in a complete array integrated with the proposed MP-CRLH phase shifters, the active reflection coefficient (ARC) is plotted and compared with the passive reflection coefficient. The corresponding results shown in Figure 14 demonstrate that the impedance matching of the antenna with the array environment remains identical to that of the single antenna at 2.45 GHz.

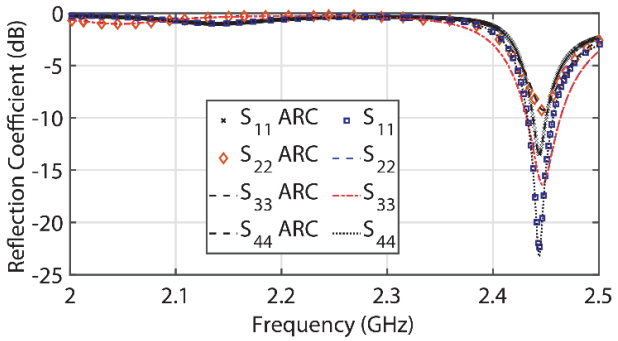

FIGURE 14. Active reflection coefficient analysis of the conformal 1x4 antenna array (radius 10 cm) integrated with MP-CRLH.

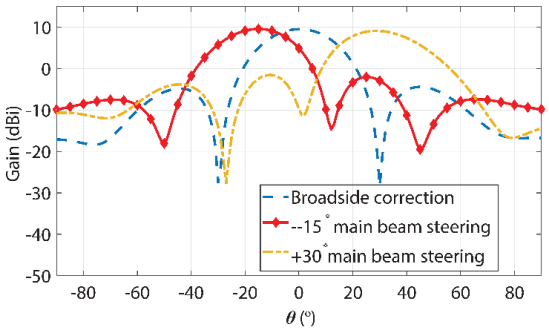

FIGURE 15. Radiation patterns of a 1 × 4 phased array for main beam steering at 0°, −1° and +3° on a planar surface.

The maximum broadside gain achieved is 9.52 dB, as shown in Figure 15, with equal phases applied to all antenna elements. Furthermore, the planar phased array is simulated for main beam steering at −15° and +30° with achieved peak gains of 9.51 dBi and 9.11 dBi, respectively, as shown in Figure 15. The reduced gain of around 0.409 dB is the scanned loss during main beam steering. For planar configuration, the required phases are with MP-CRLH phase shifters using the phase shift plots shown in Figure 5 at 2.45 GHz.

Next, for broadside and scanned radiation patterns using the cylindrical-shaped conformal array, the phase response plots in Figures 8 and 10 are utilized to achieve the

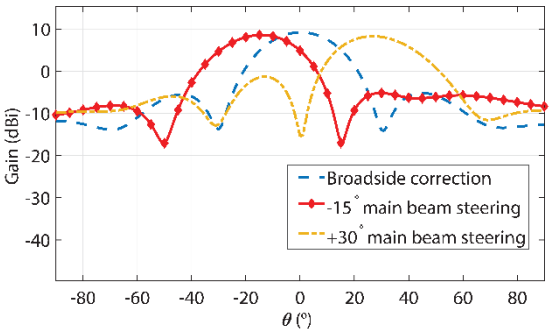

FIGURE 16. Radiation patterns of a 1 × 4 phased array for main beam steering at 0°, −15° and +30° on a conformal cylindrical surface with radius $r = 30$ cm.

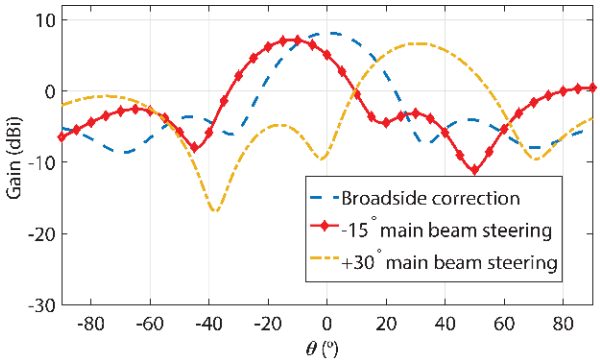

FIGURE 17. Radiation patterns of a 1 × 4 phased array for main beam steering at 0°, −15° and +30° on a conformal cylindrical surface with radius $r = 10$ cm.

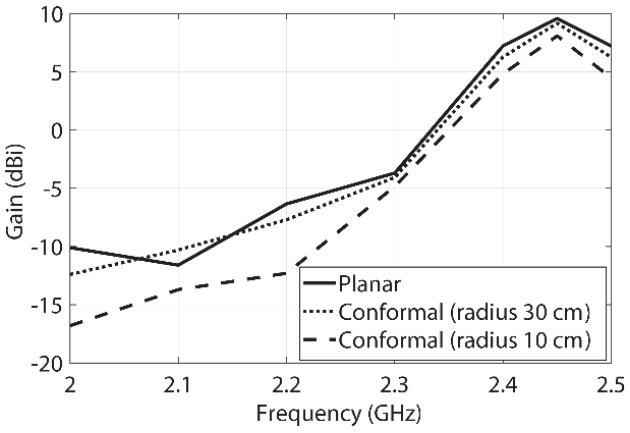

FIGURE 18. Gain vs. frequency plot of the proposed MP-CRLH integrated array in planar and conformal configurations.

desired phases. The corresponding radiation pattern plots are shown in Figures 16 and 17. The peak gain values for the broadside and scanned cases on cylindrical surfaces are given in Table 1. The required phases achieved with MP-CRLH phase shifters for the three simulation cases are given in Table 1. The peak gain difference between the planar and most conformed cases of a 10 cm conformal array for broadside, −15° and +30° scanned cases is 1.36 dB, 2.36 dB, and 2.44 dB, respectively. This gain degradation is attributed to more surface deformation, differences in antenna

TABLE 1. Phases (degrees) achieved with MP-CRLH phase shifter for planar phased array.

Scan angle (deg)	Antenna element	Calculated Phases using [20]	Phases achieved with MP-CRLH phase shifter	Activated Magnetic Particles (MP)			
				Unit Cell-1	Unit Cell-2	Unit Cell-3	Unit Cell-4
0	A_{-2}	0	110.07	1,6	1,6	1,6	1,6
	A_{-1}	0	110.07	1,6	1,6	1,6	1,6
	A_1	0	110.07	1,6	1,6	1,6	1,6
	A_2	0	110.07	1,6	1,6	1,6	1,6
-15	A_{-2}	132.26	133	4,6	1,6	1,6	1,6
	A_{-1}	-181.16	178	5,10	5,10	1,6	1,6
	A_1	-134.5	-135	5,10	4,10	4,10	5,10
	A_2	-88	-90	1-5,6-11	1-5,6-10	1-5,6-10	1-5,6-10
+30	A_{-2}	0	99	4,6	3,6	3,6	4,6
	A_{-1}	90	178	5,10	5,10	1,6	1,6
	A_1	180	-90	1-5,6-11	1-5,6-10	1-5,6-10	1-5,6-10
	A_2	270	20				

TABLE 2. Phases (degrees) achieved with MP-CRLH phase shifter for conformal phased array with $r = 30$ cm.

Scan angle	Antenna element	Calculated Phases using [31]	Phases achieved with MP-CRLH phase shifter	Activated Magnetic Particles (MP)			
				Unit Cell-1	Unit Cell-2	Unit Cell-3	Unit Cell-4
0	A_{-2}	36.4	161	4,6	4,6	4,6	4,6
	A_{-1}	0	124	2,6	2,6	2,6	2,6
	A_1	0	124	2,6	2,6	2,6	2,6
	A_2	36.4	161	4,6	4,6	4,6	4,6
-15	A_{-2}	36.4	99	9	4,9	1,6	1,6
	A_{-1}	46.58	110	1,6	1,6	1,6	1,6
	A_1	93.16	153	5,8	3,9	1,6	1,6
	A_2	175.74	-113.9	1-5,6-10	1-5,6-10	1-5,6-10	1-5,6-10
+30	A_{-2}	36	161	4,6	4,6	4,6	4,6
	A_{-1}	76	205	4,9	4,9	4,9	4,9
	A_1	152	282=-78	1-5,6-10	1-5,6-9	1-5,6-8	1-5,6-10
	A_2	264	397=37	1-5,6-7	1-5,6-8	1-5,6-10	1-5,6-10

TABLE 3. Phases (degrees) achieved with MP-CRLH phase shifter for conformal phased array with $r = 10$ cm.

Scan angle	Antenna element	Calculated Phases using [31]	Phases achieved with MP-CRLH phase shifter	Activated Magnetic Particles (MP)			
				Unit Cell-1	Unit Cell-2	Unit Cell-3	Unit Cell-4
0	A_{-2}	101.83	226	5,10	4,10	4,10	5,10
	A_{-1}	0	124	2,6	2,6	2,6	2,6
	A_1	0	124	2,6	2,6	2,6	2,6
	A_2	101.83	226	5,10	4,10	4,10	5,10
-15	A_{-2}	102	145	3,6	3,6	3,6	3,6
	A_{-1}	46.58	99	4,6	3,6	3,6	4,6
	A_1	93	135	4,9	1,6	1,6	1,6
	A_2	139	-90	1-5,6-11	1-5,6-10	1-5,6-10	1-5,6-10
+30	A_{-2}	102	99	4,6	3,6	3,6	4,6
	A_{-1}	90	-90	1-5,6-11	1-5,6-10	1-5,6-10	1-5,6-10
	A_1	180	160	4,9	4,9	1,6	1,6
	A_2	372	178	5,10	5,10	1,6	1,6

individual patterns on the conformal surface, and deviations in phases achieved with MP-CRLH phase shifters. Based on the results depicted in Figures 4-10, the proposed MP-CRLH phase shifter offer acceptable reflection coefficients,

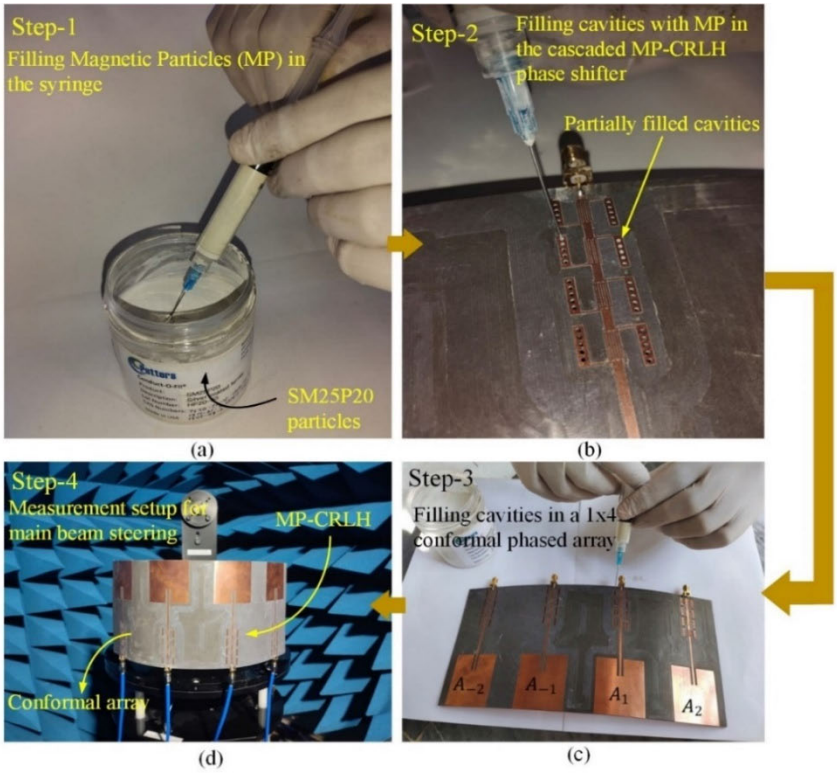

FIGURE 19. Measurements setup and procedure of 1 × 4 conformal phased array (r = 30 cm) for main beam steering at 0°, −15° and +30° (a) Filling magnetic particles in the syringe, (b) Embedding particles in the cascaded MP-CRLH phase shifter, (c) Embedding particles in the 1 × 4 phased array integrated with cascaded MP-CRLH phase shifters, (d) Complete measurement setup of the conformal phased array with integrated MP-CRLH phase shifters in an in-house anechoic chamber facility.

insertion losses, and phase responses in planar and conformal configurations. Therefore, the conformal phased array with integrated MP-CRLH phase shifters has shown promising results for broadside and scanned patterns in Figures 15-17.

Finally, the array gain vs frequency plotted in Figure 18 depicts that the gain of the proposed array remains around 9 dBi within the desired band in planar and conformal scenarios.

IV. MEASUREMENTS VALIDATION

To validate the simulation results, the 3D full-wave simulation model in Figure 10 was fabricated on a flexible Rogers RT5880 substrate ($\varepsilon_r = 2.2$, $tan\delta = 0.0009$ and thickness $h = 1.575$ mm). The prototype was conformed on a cylindrical shape having radius $r = 30$ cm. Potters Industries manufactured silver-coated micron-sized MPs were utilized in the measurements (Conduct-O-Fil®, part number SM25P20) [15]. The complete measurement procedure involves four steps. Step 1 involves filling the particles into a 5cc surgical syringe, as depicted in Figure 19(a). In step 2, the appropriate cavities are partially filled with the particles from the syringe to achieve the desired phases (see Table 1), as shown in Figure 19(b). In step 3, the top of the partially filled cavities is covered with copper tape. The resulting MP-CRLH phase shifters having MPs in them and integrated with a 1 × 4 patch antenna array are illustrated in Figure 19(c). Finally, in step 4, the complete 1 × 4 patch antenna array with MP-CRLH phase shifters is conformed on a cylindrical-shaped surface, as shown in Figure 19(d), and placed on a turntable in an anechoic chamber for the radiation pattern measurements. The radiation patterns were measured in a fully calibrated anechoic chamber (9 KHz to 20 GHz; details of the in-house chamber are in [32]). For radiation pattern measurements, a Keysight E5071C ENA Vector Network Analyzer and a Diamond Engineering automated antenna measurement system [33] were used. A broadband horn antenna (model # PE9888-11) manufactured by Pasternack is used as a source at a distance of 1.5 m away from the prototype to ensure far-field conditions. The standard cable calibration procedure available in Antenna measurement studio software [33] is utilized to minimize cable losses and calibrate the whole system, including the RF setup and rotary joints. Radiation pattern and linear gain are measured by generating the path loss and importing standard calibration data of the reference horn antenna. At the design frequency of 2.45 GHz, the measured conformal array plots for the main lobe at broadside and at scan angles of −15° and +30° are shown in Figure 20.

Reference [34] provides the video link for measurements in the in-house anechoic chamber laboratory, while [35]

TABLE 4. Comparison of the propsed design results with exsiting confromal arrays.

Reference	No. of antenna elements	Operating frequency (GHz)	Cylindrical Surface with Radius (mm)	Switching element/Material	Gain (dB)	Steering range (deg)	External DC Voltage Required
[7]	1	1.8	50, 70, 90, and 110	PIN diode	4.42	--	Yes
[8]	1	5.2	30,40	PIN diode	2.9	--	Yes
[9]	2	7.2	---	Graphene	5.5	--	Yes
[10]	4	4.99	65,95,120,240	Carbon nanotube thin-film transistors	--	0 to 27	Yes
[13]	16	61	25	SP3T semiconductor switch	16.6	-32	Yes
Proposed Work	4	2.45	100,300	Magneto-static Responsive Structures (MRSs)	9.51	+30	No

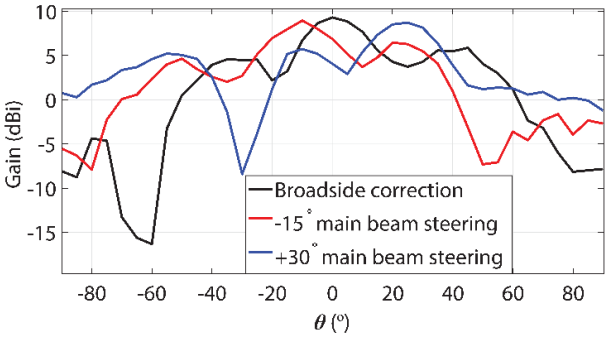

FIGURE 20. Measured radiation patterns of a 1 × 4 conformal phased arrays with integrated MP-CRLH phase shifters on a cylindrical-shaped surface with $r = 30$ cm.

provides the radiation pattern plots processed using Diamond Engineering desktop measurement software. The results are summarized in Table 1 for the full-wave simulation and measured gain. It can be deduced from the results that for a 30 cm cylindrical conformal phased array, the gain and main pattern are closely matched in simulation as well as in measured results. However, minor variations in the side lobes are due to imperfect MP-CRLH phase shifter fabrication, differences in manufactured and simulated antenna array modelling, and measurements tolerances in the anechoic chamber.

Finally, the comparison of the proposed conformal arrays having integrable MP-CRLH phase shifter with the existing conformal structures summarized in Table 4 presents notable benefits of the proposed phase shifters. Unlike the pattern reconfigurable capabilities achieved in single-element designs presented in [7] and [8] using PIN diodes, the MP-CRLH integration with the antenna array provide direct change in the pattern scanning without need of any external biasing circuitry. Reference [9] employs graphene as a switching element only in planar configuration and also requires biasing circuitry. In addition, the graphene in beam steering applications may undergo severe cracking under conformal scenarios which in return may degrade antenna performance. Furthermore, [10] and [13] provide a steering range from 0° to 27° and −32°, respectively, but still rely on an external DC source for activation. In contrast, the proposed flexible conformal phased array integrated with the proposed MP-CRLH phase shifters validated using simulations and measurements require only static magentic field without requirement of any additional biasing circuitry. Also, the direct integration of the proposed phase shifter with the antenna array element and flexibility makes it suitable for various conformal applications such as, on-body communication systems, wearable devices, flexible electronics, and aircraft communication systems.

V. CONCLUSION

In this research, a 1 × 4 flexible, fully printable, and conformal phased array antenna has been successfully demonstrated for main beam steering applications in the ISM band (2)-(4) GHz. The innovative use of micron-sized magnetic particles in a composite right/left-handed transmission line (CRLH-TL) on a flexible substrate has resulted in a variable phase shifter that can conform to non-planar surfaces, such as cylindrical-shaped surfaces in this work. The performance of the novel MPs inspired CRLH phase shifter is evaluated on a flexible Rogers RT5880 substrate for a 1 × 4 conformal phased array. It is shown that the proposed phase shifter can be used in both planar and conformal shapes with acceptable reflection coefficients, insertion losses, and phase responses. Furthermore, a 1 × 4 conformal patch array integrated the proposed MP-CRLH phase shifters has been demonstrated for main beam steering at 0°, −15°, and +30° at 2.45 GHz in simulations as well as in measurements. This study and experimental validations paved the way for future research in the fields of flexible electronics,

conformal microwave devices, wearable devices, and aircraft communication systems. Possible future research includes exploring the proposed phase shifter for complex conformal shapes and 2D conformal phased arrays.

REFERENCES

[1] J. J. Adams, E. B. Duoss, T. F. Malkowski, M. J. Motala, B. Y. Ahn, R. G. Nuzzo, J. T. Bernhard, and J. A. Lewis, "Conformal printing of electrically small antennas on three-dimensional surfaces," *Adv. Mater.*, vol. 23, no. 11, pp. 1335–1340, 2011.

[2] H. Xu, B.-Z. Zhang, J.-P. Duan, J. Cui, Y. Xu, Y. Tian, L. Yan, M. Xiong, and Q. Jia, "Wide solid angle beam-switching conical conformal array antenna with high gain for 5G applications," *IEEE Antennas Wireless Propag. Lett.*, vol. 17, no. 12, pp. 2304–2308, Dec. 2018.

[3] H. Xu, J. Cui, J. Duan, B. Zhang, and Y. Tian, "Versatile conical conformal array antenna based on implementation of independent and endfire radiation for UAV applications," *IEEE Access*, vol. 7, pp. 31207–31217, 2019.

[4] Y. Xia, B. Muneer, and Q. Zhu, "Design of a full solid angle scanning cylindrical-and-conical phased array antennas," *IEEE Trans. Antennas Propag.*, vol. 65, no. 9, pp. 4645–4655, Sep. 2017.

[5] Q. Jia, H. Xu, M. F. Xiong, B. Zhang, and J. Duan, "Omnidirectional solid angle beam-switching flexible array antenna in millimeter wave for 5G micro base station applications," *IEEE Access*, vol. 7, pp. 157027–157036, 2019.

[6] J. Lei, J. Yang, X. Chen, Z. Zhang, G. Fu, and Y. Hao, "Experimental demonstration of conformal phased array antenna via transformation optics," *Sci. Rep.*, vol. 8, no. 1, p. 3807, Feb. 2018.

[7] M.-C. Tang, B. Zhou, Y. Duan, X. Chen, and R. W. Ziolkowski, "Pattern-reconfigurable, flexible, wideband, directive, electrically small near-field resonant parasitic antenna," *IEEE Trans. Antennas Propag.*, vol. 66, no. 5, pp. 2271–2280, May 2018.

[8] B. Mohamadzade, R. B. V. B. Simorangkir, R. M. Hashmi, R. Gharaei, A. Lalbakhsh, S. Shrestha, M. Zhadobov, and R. Sauleau, "A conformal, dynamic pattern-reconfigurable antenna using conductive textile-polymer composite," *IEEE Trans. Antennas Propag.*, vol. 69, no. 10, pp. 6175–6184, Oct. 2021.

[9] Z.-P. Chen, Z.-G. Liu, L. Ju, and W.-B. Lu, "Beam scanning conformal antenna array with planar integrated phase shifter based on graphene," *J. Mater. Sci., Mater. Electron.*, vol. 33, no. 17, pp. 14032–14042, Jun. 2022.

[10] D. T. Pham, H. Subbaraman, M. Y. Chen, X. Xu, and R. T. Chen, "Light weight and conformal 2-bit, 1×4 phased-array antenna with CNT-TFT-based phase shifter on a flexible substrate," *IEEE Trans. Antennas Propag.*, vol. 59, no. 12, pp. 4553–4558, Dec. 2011.

[11] C. Fan, B. Wu, R. Song, Y. Zhao, Y. Zhang, and D. He, "Electromagnetic shielding and multi-beam radiation with high conductivity multilayer graphene film," *Carbon*, vol. 155, pp. 506–513, Dec. 2019.

[12] C. Fan, B. Wu, Y. Hu, Y. Zhao, and T. Su, "Millimeter-wave pattern reconfigurable Vivaldi antenna using tunable resistor based on graphene," *IEEE Trans. Antennas Propag.*, vol. 68, no. 6, pp. 4939–4943, Jun. 2020.

[13] V. Semkin, F. Ferrero, A. Bisognin, J. Ala-Laurinaho, C. Luxey, F. Devillers, and A. V. Räisänen, "Beam switching conformal antenna array for mm-wave communications," *IEEE Antennas Wireless Propag. Lett.*, vol. 15, pp. 28–31, 2016.

[14] A. Li, S.-W. Qu, and S. Yang, "Conformal array antenna for applications in wide-scanning phased array antenna systems," *IEEE Antennas Wireless Propag. Lett.*, vol. 21, no. 9, pp. 1762–1766, Sep. 2022.

[15] *Potters Industries LLC*. Accessed: Mar. 27, 2024. [Online]. Available: http://www.pottersbeads.com/

[16] C. Caloz and T. Itoh, *Electromagnetic Metamaterials: Transmission Line Theory and Microwave Applications*. Hoboken, NJ, USA: Wiley, 2005.

[17] M. Ayaz and I. Ullah, "A planar metamaterial transmission line phase shifter with embedded silver-coated ferrite particles," in *Proc. IEEE Int. Conf. Sensors Nanotechnol. (SENNANO)*, Sep. 2023, pp. 29–32.

[18] W. Khalil, M. Ayaz, and I. Ullah, "A terahertz frequency reconfigurable microstrip patch antenna using micron-sized silver-coated ferrite particles as switching elements," in *Proc. IEEE Int. Conf. Sensors Nanotechnol. (SENNANO)*, Sep. 2023, pp. 41–44.

[19] M. Ayaz and I. Ullah, "Designing a conformal metamaterial transmission line phase shifter with embedded micron-sized magnetic particles," in *Proc. IEEE Int. Conf. Sensors Nanotechnol. (SENNANO)*, Sep. 2023, pp. 33–36.

[20] M. Ayaz and I. Ullah, "A phased array antenna with novel composite right/left-handed (CRLH) phase shifters for Wi-Fi 6 communication systems," *Appl. Sci.*, vol. 13, no. 4, p. 2085, Feb. 2023.

[21] M. Ayaz, A. Iftikhar, B. D. Braaten, W. Khalil, and I. Ullah, "A composite right/left-handed phase shifter-based cylindrical phased array with reinforced particles responsive to magneto-static fields," *Electronics*, vol. 12, no. 2, p. 306, Jan. 2023.

[22] M. Ayaz and I. Ullah, "A singly curved conformal phased array with integrated particles-based CRLH phase shifters," *Electron. ETF*, vol. 27, no. 2, pp. 43–49, Dec. 2023.

[23] Q. Zhu, C. Gong, and H. Xin, "Design of high power capacity phase shifter with composite right/left-handed transmission line," *Microw. Opt. Technol. Lett.*, vol. 54, no. 1, pp. 119–124, 2012.

[24] A. Iftikhar, J. Parrow, S. Asif, A. Fida, J. Allen, M. Allen, B. Braaten, and D. Anagnostou, "Characterization of novel structures consisting of micron-sized conductive particles that respond to static magnetic field lines for 4G/5G (sub-6 GHz) reconfigurable antennas," *Electronics*, vol. 9, no. 6, p. 903, May 2020.

[25] D. M. Pozar, *Microwave Engineering*. Hoboken, NJ, USA: Wiley, 2011.

[26] A. Iftikhar, S. M. Asif, J. M. Parrow, J. W. Allen, M. S. Allen, A. Fida, and B. D. Braaten, "Changing the operation of small geometrically complex EBG-based antennas with micron-sized particles that respond to magneto-static fields," *IEEE Access*, vol. 8, pp. 78956–78964, 2020.

[27] A. Iftikhar, J. Parrow, S. Asif, J. Allen, M. Allen, and B. D. Braaten, "Improving the efficiency of a reconfigurable microstrip patch using magneto-static field responsive structures," *Electron. Lett.*, vol. 52, no. 14, pp. 1194–1196, Jul. 2016.

[28] A. Iftikhar, J. Parrow, S. Asif, B. D. Braaten, J. Allen, M. Allen, and B. Wenner, "On using magneto-static responsive particles as switching elements to reconfigure microwave filters," in *Proc. IEEE Int. Conf. Electro Inf. Technol. (EIT)*, May 2016, pp. 0192–0195.

[29] J. M. Parrow, A. Iftikhar, S. M. Asif, J. W. Allen, M. S. Allen, B. R. Wenner, and B. D. Braaten, "On the bandwidth of a microparticle-based component responsive to magnetostatic fields," *IEEE Trans. Electromagn. Compat.*, vol. 59, no. 4, pp. 1053–1059, Aug. 2017.

[30] J. M. Parrow, A. Iftikhar, S. M. Asif, B. D. Braaten, J. W. Allen, M. S. Allen, and B. R. Wenner, "On controlling the propagation characteristics of microstrip transmission lines using embedded micron-sized particles and static h-fields," in *Proc. IEEE Int. Symp. Antennas Propag. USNC/URSI Nat. Radio Sci. Meeting*, Jul. 2017, pp. 2269–2270.

[31] B. D. Braaten, S. Roy, S. Nariyal, M. Al Aziz, N. F. Chamberlain, I. Irfanullah, M. T. Reich, and D. E. Anagnostou, "A self-adapting flexible (SELFLEX) antenna array for changing conformal surface applications," *IEEE Trans. Antennas Propag.*, vol. 61, no. 2, pp. 655–665, Feb. 2013.

[32] *Signal Absorber Installation*. Accessed: Jun. 3, 2024. [Online]. Available: https://www.cuiatd.edu.pk/electrical-computer-engineering/research-project-cba/signal-absorber-installation/

[33] *Diamond Engineering Automated Measurement System*. Accessed: Jun. 3, 2024. [Online]. Available: https://www.diamondeng.net/support/documents/damsmanual.pdf

[34] (Jan. 15, 2024). *Irfan Khan. MP CRLH Conformal Phase Array*. Accessed: Jun. 3, 2024. [Online]. Available: https://www.youtube.com/watch?v=SWl2LelewuY

[35] *Research Projects. Design and Development of Conformal Beamforming Array (CBA) for Aerial Platforms-Plots*. Accessed: Jun. 3, 2024. [Online]. Available: https://www.cuiatd.edu.pk/electrical-computer-engineering/research-project-cba/plots/

MUHAMMAD AYAZ received the bachelor's degree in electronics engineering from the University of Engineering and Technology Peshawar, Abbottabad Campus, in 2013, the master's degree in electrical engineering from COMSATS University Islamabad, Abbottabad Campus, in 2017, where he is currently pursuing the Ph.D. degree in electrical engineering. His interests include research on nanoparticles for electromagnetic applications.

IRFAN ULLAH received the Ph.D. degree in electrical and computer engineering from North Dakota State University, Fargo, ND, USA, in 2014. He is an Associate Professor with the Electrical and Computer Engineering Department, COMSATS University Islamabad, Abbottabad Campus. His research interests include beamforming arrays, machine learning in antenna arrays, electromagnetic metamaterials, and topics in EMC.

ADNAN IFTIKHAR (Senior Member, IEEE) received the B.S. degree in electrical engineering (telecommunication) from COMSATS University Islamabad (CUI), Islamabad, Pakistan, in 2008, the M.S. degree in personal mobile and satellite communication from the University of Bradford, Bradford, U.K., in 2010, and the Ph.D. degree in electrical and computer engineering from North Dakota State University (NDSU), Fargo, ND, USA, in 2016. He is currently a tenured Associate Professor with the Department of Electrical Engineering, CUI. He was also a Marie Skłodowska-Curie Fellow and a Research Executive with Hacettepe University, Ankara, Turkey, where he carried out research on flexible substrate for antenna designing in biomedical and wearable applications. He has established various RF research facilities with CUI. He has authored or co-authored 85 journals and conference publications. He was a recipient of various national and international funding's. His research interests include reflectarray antennas, multilayer antennas, wearable biomedical antennas, frequency selective surfaces, and metamaterial absorbers. He has been actively engaged as a reviewer of RF and antenna related international journals.

SYED MUZAHIR ABBAS (Senior Member, IEEE) received the B.Sc. degree in electrical (telecommunication) engineering from the COMSATS Institute of Information Technology (CIIT), Islamabad, Pakistan, in 2006, the M.Sc. degree in computer engineering from the Center for Advanced Studies in Engineering (CASE), Islamabad, in 2009, and the Ph.D. degree in electronics engineering from Macquarie University, North Ryde, NSW, Australia, in 2016. He has been a Transmission Engineer with Alcatel-Lucent, Pakistan; a RF Engineer with CommScope, Australia; and a Senior Antenna Design Engineer and a Senior Principal Engineer with Benelec Technologies, Australia. He has lectured various courses with CIIT, and in Australia with Western Sydney University, Macquarie University, and The University of Sydney. Currently, he is a Lead Antenna Design Engineer with GME, Australia. He has been a Visiting Researcher with the ElectroScience Laboratory, The Ohio State University, USA; and the Queen Mary University of London, U.K. His research interests include base station antennas, 5G antennas, mmWave antennas, 3-D printed technology, metamaterials and metasurfaces, high impedance surfaces (HIS), frequency selective surfaces (FSS), electromagnetic bandgap structures (EBG), artificial magnetic conductor (AMC), beam steering, UWB, multiband antennas, flexible/embroidered antennas, CNT yarns, CNT/graphene-based antennas, reconfigurable antennas/electronics, and the development of antennas for UWB, VHF, UHF, and WBAN applications. He has received several prestigious awards and fellowships, including the 2020 IEEE 5G World Forum Best Paper Award; the 2019 IEEE NSW Outstanding Young Professional Award; the 2018 Young Scientist Award (Commission B–Field and Waves) from the International Union of Radio Science (URSI); the 2013 CSIRO Postgraduate Fellowship; the 2012 iMQRES Award for Ph.D.; and the Research Productivity Awards from CIIT, Pakistan, in 2012 and 2010.

BENJAMIN D. BRAATEN (Senior Member, IEEE) received the B.S. and M.S. degrees in electrical engineering and the Ph.D. degree in electrical and computer engineering from North Dakota State University (NDSU), Fargo, ND, USA, in 2002, 2005, and 2009, respectively. In 2009 Fall, he held a postdoctoral research position with the South Dakota School of Mines and Technology, Rapid City, SD, USA. In 2009 Fall, he joined the Faculty of the Electrical and Computer Engineering Department, NDSU, and was promoted to an Associate Professor with tenure, in 2015. He is a department chair of the ECE Department, NDSU. He has authored or co-authored more than 100 reviewed journals and conference publications, several book chapters on the design of antennas for radiofrequency identification, and holds one U.S. patent on wireless pacing of the human heart. His research interests include printed antennas, conformal self-adapting antennas, microwave devices, topics in EMC, topics in BIO EM, and methods in computational electromagnetics. He is a member of the National Honorary Mathematical Society PI MU EPSILON. He received the College of Engineering and Architecture Graduate Researcher of the Year and College of Engineering and Architecture Graduate Teacher of the Year Awards. He serves as an Associate Editor for IEEE Antennas and Wireless Propagation Letters.

SHAHID KHATTAK received the Bachelor of Science degree in electrical engineering from the University of Engineering and Technology Peshawar, Pakistan, in 1993, the Master of Science degree in electrical engineering, with a specialization in communications and signal processing from Purdue University, USA, in 1997, and the Ph.D. degree in electrical engineering from the Technische Universität Dresden, Germany, in 2008. His research interests include the forefront of mobile communication systems, particularly beyond 5G technologies. His work emphasizes base station cooperation and spectrum efficiency, aiming to enhance the performance and reliability of next-generation networks. Additionally, he has conducted extensive research on bio-inspired algorithms, deep learning, and conformal beamforming antennas, and contributing significantly to advancements in these areas.

MOATH ALATHBAH received the Ph.D. degree from Cardiff University, U.K. He is currently an Assistant Professor with King Saud University, Saudi Arabia. His research interests include the development of photoelectronic; integrated electronic active and passive discrete devices; the design, fabrication, and characterization of MMIC; RF and THz components; smart antennas; microstrip antennas; microwave filters; metamaterials; 5G antennas; MIMO antennas miniaturized multiband/wideband antennas; and microwave/millimeter components using micro and nano technology.